REGULAR ARTICLE

blood advances

Combined GLUT1 and OXPHOS inhibition eliminates acute myeloid leukemia cells by restraining their metabolic plasticity

Maria Rodriguez-Zabala,[1,2] Ramprasad Ramakrishnan,[1,2] Katrin Reinbach,[1,2] Somadri Ghosh,[1,2] Leal Oburoglu,[2,3] Antoni Falqués-Costa,[1] Kishan Bellamkonda,[1] Mats Ehinger,[4] Pablo Peña-Martínez,[1] Noelia Puente-Moncada,[1] Henrik Lilljebjörn,[1] Jörg Cammenga,[2,5] Cornelis Jan Pronk,[2,6] Vladimir Lazarevic,[5] Thoas Fioretos,[1] Anna K. Hagström-Andersson,[1] Niels-Bjarne Woods,[2,3] and Marcus Järås[1,2]

[1]Division of Clinical Genetics, [2]Lund Stem Cell Center, and [3]Division of Molecular Medicine and Gene Therapy, Lund University, Lund, Sweden; and [4]Division of Pathology, Department of Clinical Sciences, [5]Department of Hematology, Oncology and Radiation Physics, and [6]Childhood Cancer Center, Skåne University Hospital, Lund, Sweden

Key Points

- GLUT1 is essential for energy metabolism of murine *MLL::AF9* LSCs in the bone marrow microenvironment.
- GLUT1 and OXPHOS inhibition eliminates human AML cells.

Acute myeloid leukemia (AML) is initiated and propagated by leukemia stem cells (LSCs), a self-renewing population of leukemia cells responsible for therapy resistance. Hence, there is an urgent need to identify new therapeutic opportunities targeting LSCs. Here, we performed an in vivo CRISPR knockout screen to identify potential therapeutic targets by interrogating cell surface dependencies of LSCs. The facilitated glucose transporter type 1 (GLUT1) emerged as a critical in vivo metabolic dependency for LSCs in a murine *MLL::AF9*–driven model of AML. GLUT1 disruption by genetic ablation or pharmacological inhibition led to suppression of leukemia progression and improved survival of mice that received transplantation with LSCs. Metabolic profiling revealed that *Glut1* inhibition suppressed glycolysis, decreased levels of tricarboxylic acid cycle intermediates and increased the levels of amino acids. This metabolic reprogramming was accompanied by an increase in autophagic activity and apoptosis. Moreover, *Glut1* disruption caused transcriptional, morphological, and immunophenotypic changes, consistent with differentiation of AML cells. Notably, dual inhibition of GLUT1 and oxidative phosphorylation (OXPHOS) exhibited synergistic antileukemic effects in the majority of tested primary AML patient samples through restraining of their metabolic plasticity. In particular, *RUNX1*-mutated primary leukemia cells displayed striking sensitivity to the combination treatment compared with normal $CD34^+$ bone marrow and cord blood cells. Collectively, our study reveals a GLUT1 dependency of murine LSCs in the bone marrow microenvironment and demonstrates that dual inhibition of GLUT1 and OXPHOS is a promising therapeutic approach for AML.

Introduction

Acute myeloid leukemia (AML) is a heterogeneous hematological malignancy with a 5-year survival rate of <30%.[1] This dismal outcome has been attributed to an inability of conventional chemotherapy to

Submitted 9 February 2023; accepted 12 July 2023; prepublished online on *Blood Advances* First Edition 28 July 2023. https://doi.org/10.1182/bloodadvances.2023009967.

RNA-sequencing data are available at the Gene Expression Omnibus repository under accession number GSE209636.

Data are available on request from the corresponding author, Marcus Järås (marcus.jaras@med.lu.se).

The full-text version of this article contains a data supplement.

eradicate leukemia stem cells (LSCs), a distinct subpopulation that drives disease initiation, perpetuation, and relapse.[2,3]

Based on the potential therapeutic value of targeting LSCs, multiple strategies have focused on exploiting LSC-specific vulnerabilities to improve outcomes of patients with AML. The distinct metabolic properties of LSCs compared with normal hematopoietic cells have recently prompted interest in targeting energy metabolism as an antileukemic therapy.[4,5] However, antileukemic effects are often hampered by metabolic adaptation and patient heterogeneity.[6] Understanding the mechanisms underlying metabolic dependencies of LSCs and exploiting them therapeutically may provide new treatment strategies.

To identify physiologically relevant dependencies, we, and others, have performed in vivo CRISPR-Cas9 screens to uncover LSC vulnerabilities within the bone marrow niche.[7-9] Although many screens reveal critical dependencies for leukemia maintenance and progression, these candidates are often not suitable as therapeutic targets. Cell surface proteins, however, have extracellular accessibility for pharmacological intervention and, thus, provide a basis for many types of targeted therapies.[10] In particular, identification of cell surface antigens required for survival of LSCs may be therapeutically relevant because they are less likely to be downregulated as a resistance mechanism.

Here, we performed an in vivo CRISPR-Cas9 dropout screen in a murine *MLL::AF9 (KMT2A::MLLT3)*-driven AML model and identified the facilitated glucose transporter type 1 (GLUT1) as the top-scoring dependency of LSCs. Genetic and pharmacological inhibition of GLUT1 compromised LSC activity by disrupting energy metabolism, accompanied by enhanced apoptosis, differentiation, and autophagic activity. In human AML cell lines and in the majority of tested samples from patients with AML, inhibition of GLUT1 and oxidative phosphorylation (OXPHOS) synergistically impaired leukemia cell survival while having milder effects on normal cells. Our study provides a deeper understanding of how GLUT1 regulates metabolic processes of leukemia cells, findings that may translate into improved therapies in AML.

Methods

Murine *MLL::AF9* leukemia model

The murine *MLL::AF9* AML model expressing Cas9 was previously generated.[11] Leukemia cells were serially propagated in sublethally irradiated C57BL/6 recipient mice, as previously described.[11] *MLL::AF9* leukemia cells were harvested from the bone marrow and enriched for LSCs by isolating the receptor tyrosine kinase$^+$ (c-Kit$^+$) cell population, and cultured in Stemspan (StemCell Technologies) containing 1% penicillin/streptomycin (Cytvia), supplemented with murine interleukin-3, murine stem cell factor, and human interleukin-6 (Peprotech).[7]

CRISPR library construction and screen

A lentiviral library containing 5798 single-guide RNAs (sgRNAs) targeting 961 genes encoding cell surface proteins was generated, as previously described.[12] The genes targeted were selected from the Cell Surface Protein Atlas database followed by manual curation.[10] In vivo pooled CRISPR dropout screening was performed using c-Kit$^+$ *MLL::AF9* leukemia cells, as previously described.[7]

RNA sequencing

Global gene expression profiling was performed on sorted green fluorescent protein–positive (GFP$^+$) *MLL::AF9* leukemia cells 3 days after transduction with Glut1 sgRNAs or a nontargeting control. Data have been deposited under the accession number GSE209636.

Mass spectrometry–based metabolomics

Absolute quantification of the tricarboxylic acid (TCA) cycle intermediates and amino acids was performed by gas chromatography coupled with triple quadrupole mass spectrometry. Sugar-phosphate metabolites were quantified by liquid chromatography coupled with triple quadrupole mass spectrometry.

Statistical analysis

Statistical analyses between Glut1 sgRNA and nontargeting control groups were performed using 1-way analysis of variance (ANOVA) with Dunnett's correction, and differences between drug and dimethyl sulfoxide (DMSO)-treated groups using unpaired 2-tailed Student *t* test, unless otherwise indicated. Data are presented as the mean ± standard deviation, with at least 3 biological replicates, unless otherwise stated. $*P < .05$, $**P < .01$, $***P < .001$, and $****P < .0001$.

Refer to supplemental Table 1 for a list of antibodies used, supplemental Table 2 for sgRNA sequences, and supplemental Information for further methodology details.

Results

In vivo CRISPR-Cas9 screening identifies GLUT1 as a novel regulator of *MLL::AF9*–driven leukemia

To identify cell surface molecules that are critical for the growth and survival of LSCs in AML, we generated a CRISPR library targeting 961 genes encoding cell surface proteins. The screen was performed using an *MLL::AF9*–driven AML mouse model enriched for stem cell activity and with a rapid disease progression.[7,13,14] The pooled sgRNA library was lentivirally transduced into serially propagated Cas9$^+$ c-Kit$^+$ dsRed$^+$ *MLL::AF9* leukemia cells and transplanted into sublethally irradiated mice (Figure 1A).[7,11] *Glut1,* which encodes GLUT1, was identified as the top-scoring hit, with 6 of 6 sgRNAs depleted >10-fold (Figure 1B-C; supplemental Figure 1A-D; supplemental Tables 2 and 3). Furthermore, among the 20 genes with the strongest depletion scores were known AML stem cell dependencies, including *Cxcr4, Cd47,* and *Hoxa9,* the latter included as a positive control, confirming the robustness of the screen.[7,15-17] Other genes associated with survival of leukemia cells such as *Gnb211* and *Tmem30a* also scored as strong in vivo dependencies (Figure 1B; supplemental Table 3).[18,19]

GLUT1 is required for *MLL::AF9*–driven AML cell growth and survival

Growing evidence suggests that AML cells rely on unique and exploitable metabolic properties for survival, thus making glucose transporters promising therapeutic targets.[4] To examine the relevance of GLUT1 in AML, we investigated the expression of *GLUT1* (also known as *SLC2A1*) in a cohort of CD34$^+$ hematopoietic stem and myeloid progenitor cells from the bone marrow of healthy donors (n = 22),[20,21] and in 5 cohorts of patients with AML (n =

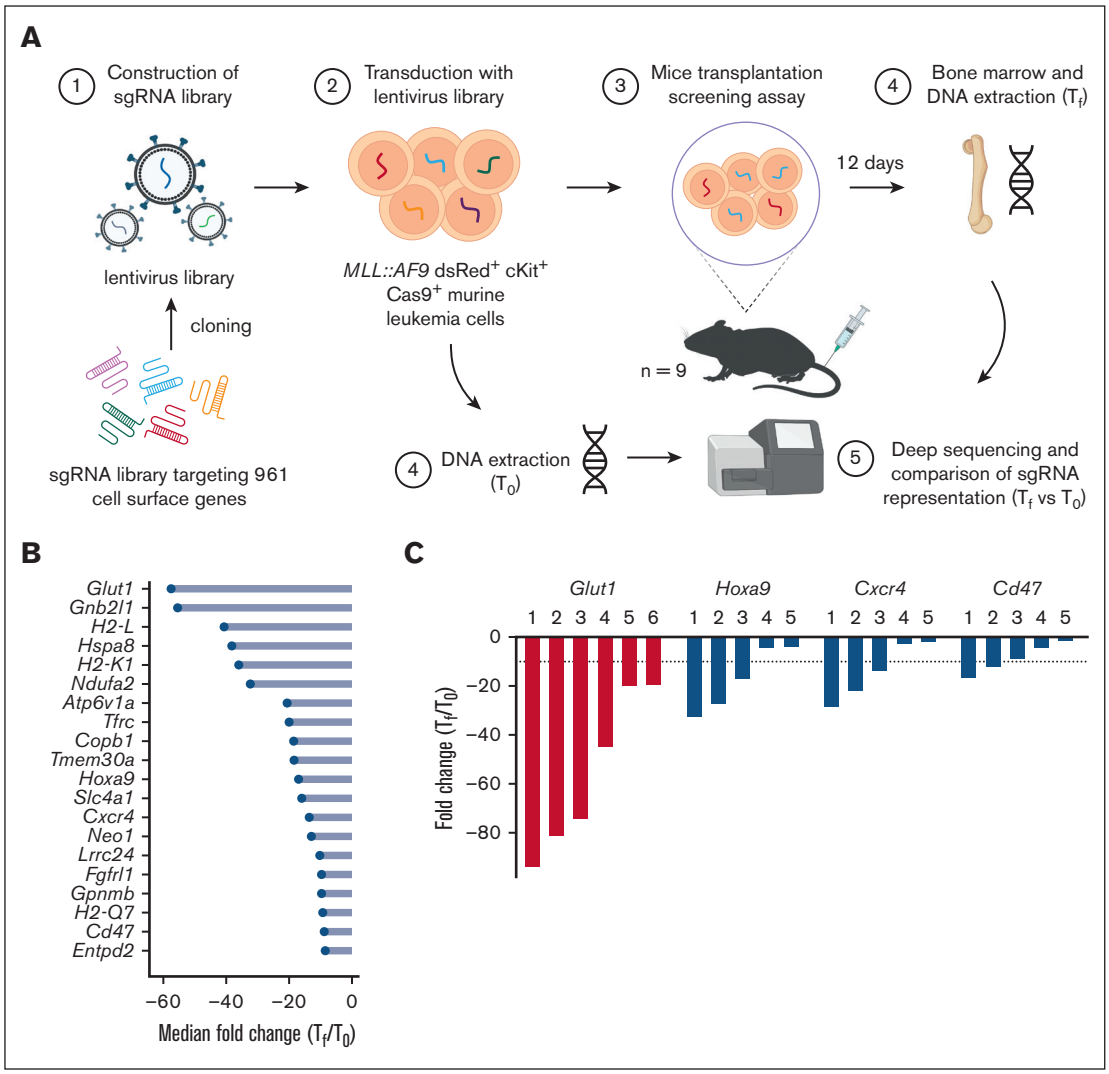

Figure 1. In vivo CRISPR-Cas9 screening identifies an essential role for *Glut1* in *MLL::AF9*–driven AML. (A) Schematic representation of the experimental design for the pooled in vivo CRISPR screen in *MLL::AF9* c-Kit$^+$ leukemia cells (n = 9 mice). (B) Bar plot of normalized median fold change of sgRNAs for the 20 genes with the strongest depletion scores in the screen. Fold change in sgRNA representation in leukemic cells harvested from the bone marrow was calculated as the number of reads after 12 days in vivo (final time point [T_f]) relative to input representation (initial time point [T_0]). (C) Waterfall plot showing the normalized fold change of individual sgRNAs for the top regulator *Glut1* and 3 known regulators of *MLL::AF9* AML (*Hoxa9, Cxcr4,* and *Cd47*). A fold change of 10 was used to define depleted sgRNAs, denoted with a dotted line. Illustration in panel A created using BioRender. See also supplemental Figure 1 and supplemental Table 3.

1706) using the BloodSpot tool.[22-27] *GLUT1* was expressed across all AML subtypes, suggesting that the GLUT1 dependency is not confined to a specific AML subtype (supplemental Figure 2A). A pediatric cohort of patients with *MLL*-rearranged AML (n = 9) or acute lymphoblastic leukemia (n = 53) also showed clear *GLUT1* expression (supplemental Figure 2B).[28] Similarly, in murine *MLL::AF9* leukemia cells, GLUT1 levels were markedly upregulated in primary LSC-enriched c-Kit$^+$ and leukemic granulocyte-monocyte progenitor populations compared with their normal bone marrow counterparts (Figure 2A; supplemental Figure 2C-D). Compared with the other class I facilitative glucose transporters (*Glut2, Glut3*, and *Glut4*), *Glut1* expression was >20-fold higher (supplemental Figure 2E).

To study the mechanistic basis for the GLUT1 dependency of AML cells, *Glut1* was knocked down in murine *MLL::AF9* cells using the 3 highest scoring sgRNAs targeting *Glut1* in the screen (sgRNA1-3) (supplemental Table 2). High CRISPR-mediated editing efficiency was confirmed by deep sequencing, which translated into significant knockdown at the protein level (Figure 2B-C; supplemental Figure 2F-G). Consistent with the screening results, sgRNA-mediated ablation of *Glut1* in c-Kit$^+$ *MLL::AF9* leukemia cells transplanted into mice led to a robust depletion of GFP$^+$ (sgRNA-expressing) cells in the bone marrow (Figure 2D) and spleen (supplemental Figure 2H). Similarly, a rapid depletion of *Glut1* sgRNA-expressing leukemia cells was also observed over time in a competition assay ex vivo (Figure 2E). These findings indicate that GLUT1 regulates critical intracellular mechanisms driving myeloid leukemia progression.

To assess whether *Glut1* is essential for LSCs, recipient mice received transplantation with sorted GFP$^+$ c-Kit$^+$ *MLL::AF9* cells

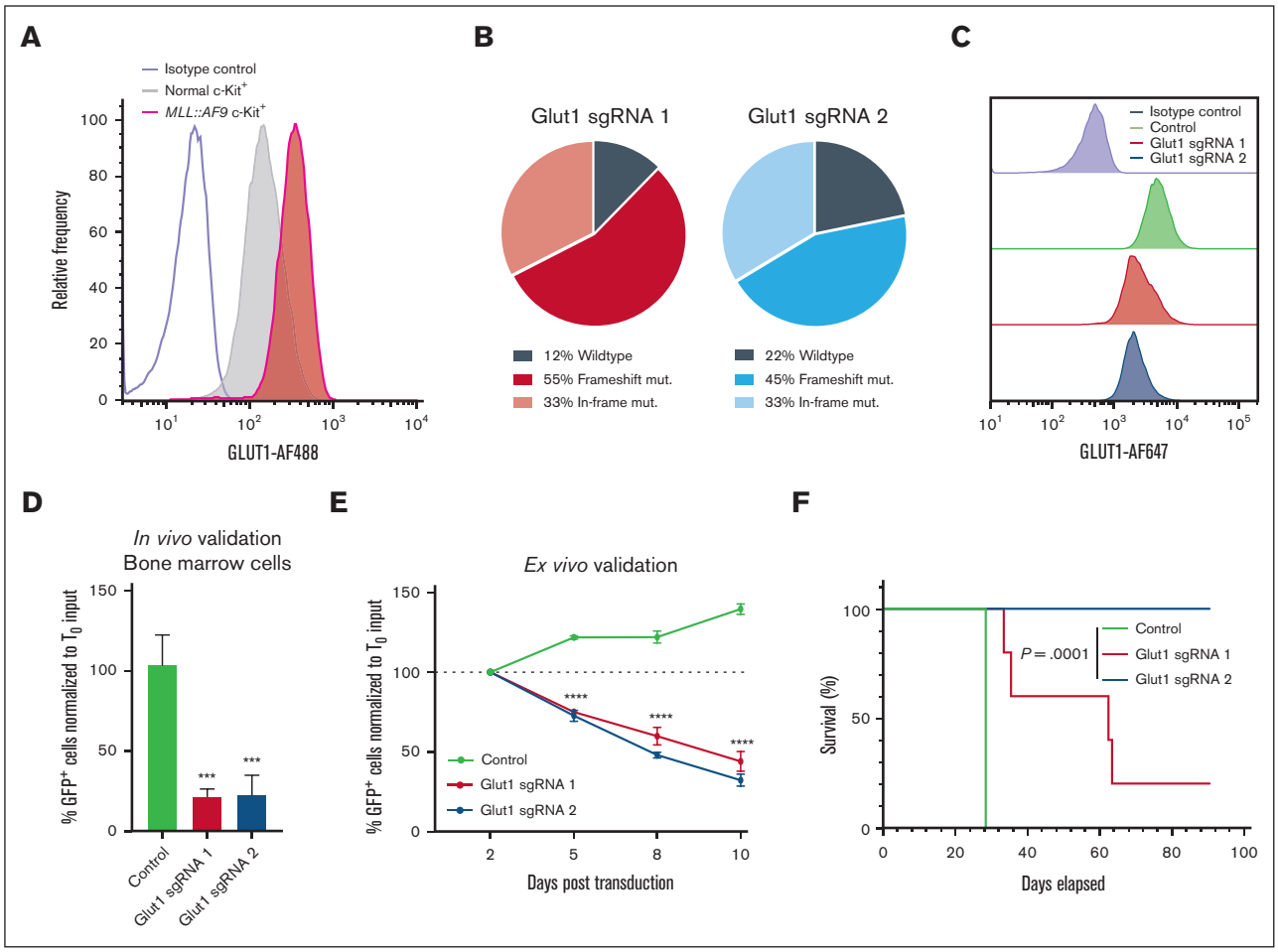

Figure 2. GLUT1 is required for AML cell growth and survival. (A) Flow cytometric analysis of GLUT1 expression in *MLL::AF9* LSC-enriched (c-Kit$^+$) cells and their normal bone marrow c-Kit$^+$ counterparts. In panels B to F, *MLL::AF9* cells were transduced with Glut1 sgRNAs (Glut1 sgRNA1 and sgRNA2) or a nontargeting control cloned into GFP-expressing lentiviral vectors. (B) Genetic editing in the *Glut1* locus was quantified by deep sequencing within sorted GFP$^+$ cells, 3 days after transduction. (C) Representative histogram of GLUT1 expression measured by flow cytometry within GFP$^+$ leukemia cells, 4 days after transduction. (D) Quantification of GFP$^+$ *MLL::AF9* leukemia cells in the bone marrow of mice 12 days after transplantation with c-Kit$^+$ leukemia cells transduced with Glut1 sgRNAs or nontargeting control. The percentage of GFP$^+$ cells at day 12 was normalized to the input percentage of GFP$^+$ cells before transplantation, 2 days after transduction (T_0). (E) Ex vivo competition proliferation assay as measured by the percentage of GFP$^+$ leukemia cells on day 2, 5, 8, and 10 after transduction, normalized to the input percentage at day 2 (T_0). (F) Kaplan-Meier survival analysis of mice that received transplantation with sorted GFP$^+$ leukemia cells 2 days after transduction (n = 5 mice per group; log-rank test). Data are represented as mean ± standard deviation (SD) with an n = 3, unless otherwise stated. Significance was measured by 1-way analysis of variance (ANOVA) with the following thresholds: ***$P < .001$ and ****$P < .0001$. Refer to supplemental Figure 2 and supplemental Table 2.

transduced with Glut1 sgRNA or a nontargeting control. Mice that received transplantation with *Glut1*-disrupted leukemia cells had a significantly prolonged survival, albeit with differences between the 2 Glut1 sgRNAs (Figure 2F; supplemental Figure 2I-J). Although only 1 of 5 mice that received transplantation with leukemia cells expressing Glut1 sgRNA1 survived, the recipients that received transplantation with Glut1 sgRNA2-expressing cells displayed no signs of disease (Figure 2F; supplemental Figure 2I -J). Notably, examination of the leukemic blasts harvested from recipients that received transplantation with Glut1 sgRNA1-expressing cells that succumbed to disease revealed a restored GLUT1 expression (supplemental Figure 2K-L). This observation suggests that rare AML cells either with nondeleterious editing or that had escaped *Glut1* knockdown had expanded. Overexpression of a sgRNA2-resistant *Glut1* complementary DNA rescued the effects induced by Glut1 sgRNA2, suggesting that the strong antileukemic effects of sgRNA2 were not caused by off-target effects (supplemental Figure 2M-N). Taken together, these data indicate that GLUT1 is essential for LSCs in the *MLL::AF9*–driven leukemia mouse model.

Glut1 disruption induces apoptosis and differentiation of *MLL::AF9* leukemia cells

Next, we sought to investigate the cellular mechanisms by which *Glut1* regulates leukemia progression. Whereas *Glut1* disruption did not have an effect on cell cycle status (supplemental Figure 3A), it induced poly-adenosine diphosphate (ADP) ribose polymerase (PARP) and caspase-3 activation, accompanied by late-stage apoptosis in c-Kit$^+$ *MLL::AF9* leukemia cells (Figure 3A-C). Alterations consistent with apoptosis were also

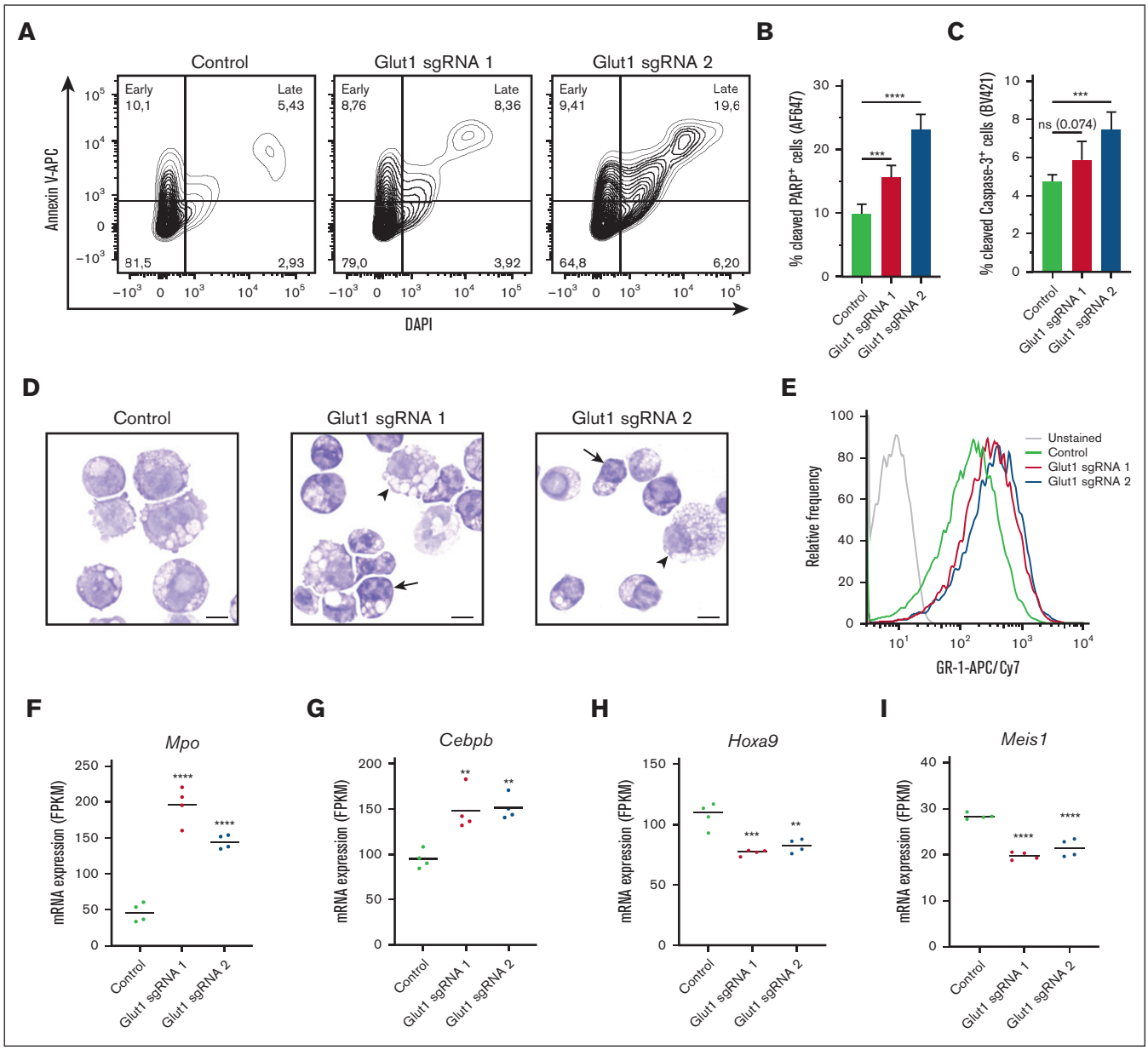

Figure 3. *Glut1* disruption induces apoptosis and differentiation of *MLL::AF9* leukemia cells. (A-E) Mechanistic investigation of *Glut1* disruption was performed in LSC-enriched (c-Kit$^+$) bone marrow–derived *MLL::AF9* cells lentivirally transduced with Glut1 sgRNAs or nontargeting control, 3 or 4 days after transduction. (A) Representative contour plots showing the percentage of early- (annexin-V$^+$ 4′,6-diamidino-2-phenylindole [DAPI]$^-$) and late-stage (annexin-V$^+$ DAPI$^+$) apoptotic cells. Flow cytometric quantification of (B) cleaved PARP and (C) cleaved caspase-3 (n = 5). (D) Representative light microscopy images of May-Grünwald Giemsa–stained *MLL::AF9* cells. Arrows delineate chromatin condensation in nuclei, and arrowheads indicate cells with more ample cytoplasm, reflecting monocytic differentiation (scale bar, 25 μm). (E) Representative histogram showing cell surface expression of GR-1, unstained shown in light gray. In panels F to I, RNA-seq was performed on sorted GFP$^+$ *MLL::AF9* cells, 3 days after transduction with either Glut1 sgRNAs or nontargeting control (n = 4). Changes in messenger RNA (mRNA) expression of (F) *Mpo*, (G) *Cebpb*, (H) *Hoxa9* and (I) *Meis1* after *Glut1* knockdown are represented as fragments per kilobase of transcript per million mapped reads (FPKM) values. Data are shown as mean ± SD (n = 3), unless otherwise stated; statistical testing was performed by 1-way ANOVA. $^{**}P < .01$; $^{***}P < .001$; and $^{****}P < .0001$. Refer to supplemental Figure 3. PARP, poly-ADP ribose polymerase; RNA-seq, RNA sequencing.

observed morphologically, as evidenced by an overall cell shrinkage and chromatin condensation in the nuclei (Figure 3D). Moreover, we observed a reduced nucleus-to-cytoplasm ratio and increased expression of the differentiation marker GR-1 consistent with myeloid differentiation (Figure 3D-E).

To gain insights into the molecular effectors regulated by GLUT1 in AML, we performed RNA sequencing of c-Kit$^+$ *MLL::AF9* leukemia cells after *Glut1* disruption. *Glut1* knockdown induced a distinct gene expression signature, herein referred to as the *Glut1* inhibition signature, with 1688 genes identified as differentially expressed

(false discovery rate [FDR] < 0.01) (supplemental Figure 3B). Gene set enrichment analysis (GSEA) revealed that genes associated with myeloid differentiation were enriched in the *Glut1* inhibition signature (supplemental Figure 3C).[29] Among the significantly upregulated genes were *Cebpb* and *Mpo*, myeloid lineage commitment markers important for late stages of myeloid differentiation (Figure 3F-G).[30,31] Furthermore, a large subset of *Hoxa* genes including *Hoxa3*, *Hoxa7*, *Hoxa9*, and *Hoxa10*, known to be critical for the self-renewal of LSCs, were significantly downregulated in *Glut1*-disrupted cells (Figure 3H; supplemental Figure 3D-F).[32] Similarly, a downregulation of *Meis1*, which cooperates with *Hoxa9* in the development of *MLL*-rearranged leukemia, was also observed (Figure 3I).[33] Taken together, molecular, morphological, and transcriptomic analyses indicate that *Glut1* ablation inhibits AML progression by inducing late-stage apoptosis and myeloid differentiation.

Glut1 inhibition suppresses glycolysis and reduces levels of TCA intermediates in leukemia cells

GSEA also revealed that the *Glut1* knockdown signature was negatively enriched for OXPHOS (FDR < 0.001) as well as for the TCA cycle (FDR = 0.061), suggesting that disruption of *Glut1*–mediated glucose uptake downregulates genes in these processes (Figure 4A-B). Given that GLUT1 is a key rate-limiting factor for glucose uptake and that knockdown leads to transcriptional changes in the genes involved in OXPHOS, we interrogated metabolic pathways directly regulated by this major glucose transporter in LSCs.

To characterize global metabolomic differences induced by *Glut1* knockdown in AML, we performed metabolomic profiling on c-Kit$^+$ *MLL::AF9* leukemia cells transduced with nontargeting control or Glut1 sgRNAs (Figure 4C-G; supplemental Table 5). After confirmation of robust group clustering using principal component analysis (supplemental Figure 4A), we assessed alterations in glycolysis, the pentose phosphate pathway (PPP), and TCA. *Glut1* disruption led to an overall suppression of glycolysis, as evidenced by a significant reduction of key glycolytic metabolites such as lactate and glucose-6-phosphate (Figure 4C-D; supplemental Table 5). We also observed downregulation of a large number of intermediates belonging to the PPP, a metabolic pathway that branches from glycolysis (Figure 4C,E; supplemental Table 5). Consistent with the GSEA data, *Glut1*-deficient leukemia cells also exhibited an overall decrease in the levels of TCA cycle intermediates (Figure 4C,F; supplemental Table 5).

As an adaptation to compromised glucose uptake, *Glut1* disruption shifted the intracellular metabolic profile of AML cells by upregulating amino acid levels (Figure 4C,G; supplemental Table 5).[34] This was accompanied by a marked increase in the transcript levels of various amino acid transporters, including those for glutamine, glutamate, aspartate, and cysteine (supplemental Figure 4B).[35] Thus, our data suggest that when glucose import via GLUT1 is compromised, AML cells use compensatory mechanisms to augment the import and/or synthesis of amino acids, which can be used as an alternative noncarbohydrate source of fuel. Another compensatory mechanism observed was a sixfold increase in *Glut3* expression, although this was not sufficient to rescue the antileukemic effect induced by *Glut1* knockdown (supplemental Figure 4C).

To functionally assess how GLUT1 regulates the bioenergetic profile of *MLL::AF9* leukemia cells, we analyzed the extracellular acidification rate (ECAR) as a measure of glycolysis via step-wise addition of glucose, oligomycin, and 2-deoxyglucose. Consistent with the metabolomic profiling, *Glut1* ablation resulted in a significant reduction in the basal ECAR in the presence of glucose (Figure 4H) and after the addition of the indicated compounds (Figure 4I). Hexokinase activity and extracellular lactate production were also compromised, indicating that GLUT1 is required for glycolysis in *MLL::AF9* leukemia cells (Figure 4J-K). In contrast, *Glut1*-disrupted leukemia cells did not exhibit significant effects on the oxygen consumption rate (OCR), indicating that mitochondrial respiration efficiency was not severely altered despite the reduced availability of TCA intermediates (Figure 4F; supplemental Figure 4D). Collectively, these data suggest that inhibiting *Glut1* suppresses the bioenergetics of *MLL::AF9* leukemia cells, and adaptation mechanisms for compensatory energy acquisition were insufficient to bypass the effects of *Glut1* inhibition.

Autophagy is induced as a metabolic adaptation in AML cells after *Glut1* disruption

As a result of nutrient starvation, cellular proteins and organelles can be degraded through autophagy, a catabolic process acting to sustain core metabolic functions and energy demands in cells. To determine the potential implication of autophagy after *Glut1* disruption, we analyzed the presence of autophagosomes and autolysosomes in c-Kit$^+$ *MLL::AF9* leukemia cells. Disruption of glucose uptake via *Glut1* knockdown in LSCs increased the amount of autophagic vacuoles and led to an accumulation of total LC3B, a canonical marker of the autophagosomal pathway (Figure 5A-B).[36] Further examination by immunoblotting revealed that *Glut1* ablation increased the levels of LC3B-I and LC3B-II in AML cells, reflecting an accumulation of both autophagophores and fully assembled autophagosomes, respectively (Figure 5C and D). Consistent with these findings, the autophagy-related 7 (*Atg7*) gene, critical in the autophagosome completion step, was upregulated in c-Kit$^+$ *MLL::AF9* cells after *Glut1* disruption (Figure 5E).[36]

In line with the hypothesis that GLUT1 inhibition induces autophagy as a metabolic adaptation to support leukemia cell survival, combined *Glut1* disruption and treatment with the autophagy inhibitor chloroquine synergistically inhibited the viability of *MLL::AF9* leukemia cells (Figure 5F).

Pharmacological inhibition of GLUT1 selectively targets *MLL::AF9* leukemia cells

To assess the feasibility of targeting GLUT1 in a therapeutic context, we performed pharmacological inhibition of GLUT1 using the highly potent and selective small molecule inhibitor BAY-876.[37] Compared with normal c-Kit$^+$ bone marrow cells, BAY-876 exhibited a selective inhibitory effect on c-Kit$^+$ *MLL::AF9* leukemia cells, with an almost sixfold lower half-maximal inhibitory concentration (Figure 6A; supplemental Figure 5A-B). Next, we performed a competitive ex vivo assay in which c-Kit$^+$ leukemia cells and normal c-Kit$^+$ cells were cocultured and treated with increasing concentrations of BAY-876. At concentrations >10 nM, leukemia cells were selectively eliminated (Figure 6B), verifying the higher sensitivity of leukemia cells to GLUT1 inhibition. To validate the mode of action of BAY-876 in leukemia cells, we confirmed that

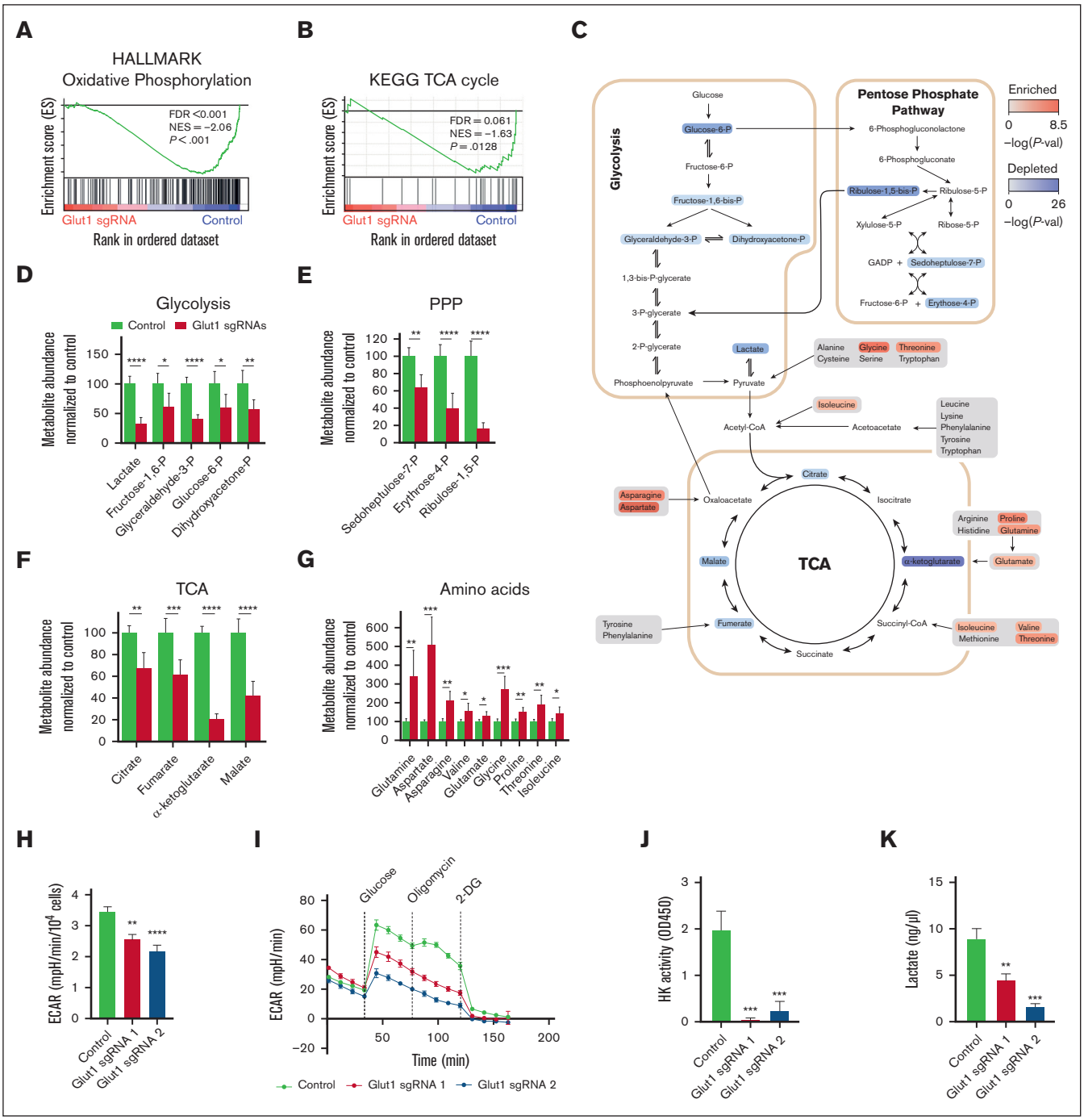

Figure 4. *Glut1* inhibition suppresses glycolysis and reduces levels of TCA intermediates in leukemia cells. (A-B) GSEA of the transcriptional signature of *Glut1* knockdown vs control obtained upon *Glut1* disruption on sorted GFP$^+$ (sgRNA-expressing) leukemia cells (n = 4). In panels C to G, targeted metabolomic analysis of sorted GFP$^+$ *MLL::AF9* cells, 4 days after transduction (Glut1 sgRNA3: n = 3; Glut1 sgRNA1, Glut1 sgRNA2, and nontargeting control: n = 4). Quantification of glycolytic and PPP metabolites by LC-MS; TCA intermediates and amino acids quantified by GC-MS. (C) Graphical representation depicting alterations in the level of key metabolites after *Glut1* knockdown. The direction of the change is encoded by color, noted as enrichment (red) and depletion (blue) in Glut1 sgRNA relative to control group. (D-G) Quantification of key metabolites in *MLL::AF9* cells with *Glut1* knockdown, with abundance normalized to cells transduced with nontargeting control. Metabolites are grouped based on their respective pathways: (D) glycolysis; (E) PPP; (F) TCA; and (G) amino acids. Significance was measured by unpaired 2-tailed Student *t* test. (H) Basal extracellular acidification rate (ECAR) in the presence of glucose, indicative of glycolytic rate (n = 4), normalized to cell number. (I) Representative glycolysis stress test assay, showing ECAR in basal conditions and after the addition of the indicated compounds in *MLL::AF9* cells (n = 4). Glucose, oligomycin, and 2-DG were injected to final concentrations of 25 mM, 1 µM, and 50 mM, respectively. (J) HK enzymatic activity evaluated by detection of NADH (ΔA_{450}), and (K) secretion levels of extracellular lactate, the end product of glycolysis, was determined by colorimetry (A_{570}). Data are shown as mean ± SD (n = 3) and statistical testing was performed by 1-way ANOVA, unless otherwise stated. *$P < .05$; **$P < .01$; ***$P < .001$; and ****$P < .0001$. Refer to supplemental Figure 4 and supplemental Table 5. 2-DG, 2-deoxyglucose; FDR, false discovery rate; GC-MS, gas chromatography–mass spectrometry; HK, hexokinase; LC-MS, liquid chromatography–mass spectrometry; NADH, nicotinamide adenine dinucleotide; NES, normalized enrichment score.

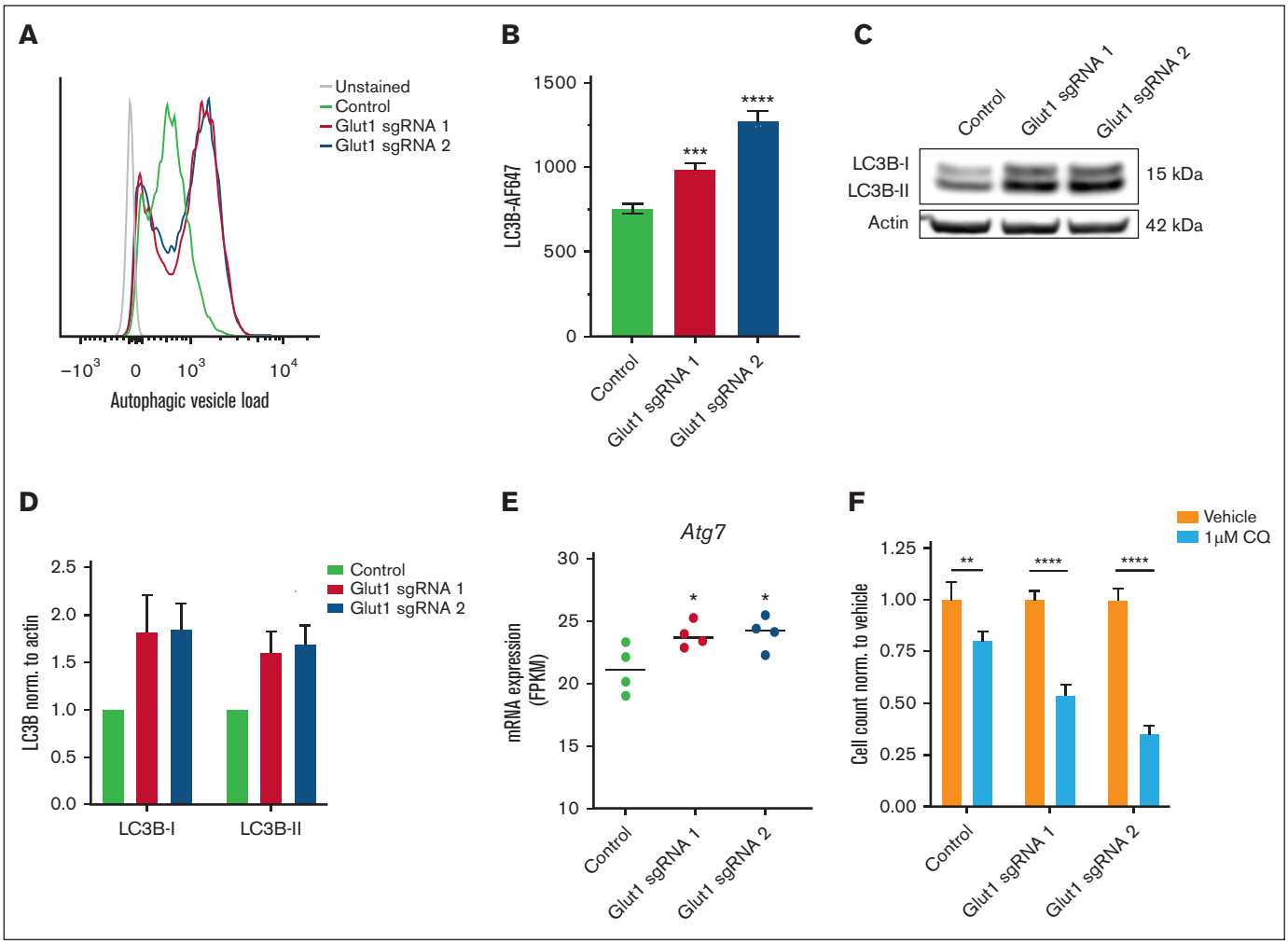

Figure 5. Autophagy is induced as a metabolic adaptation in AML cells after *Glut1* disruption. (A-D) Mechanistic investigation of *Glut1* disruption was performed in LSC-enriched (c-Kit$^+$) bone marrow–derived *MLL::AF9* cells, 4 days after transduction. (A) Representative histograms showing flow cytometric quantification of autophagic vesicle load (autophagosomes and autolysosomes) using the cell-permeant aliphatic Autophagy Probe Red. Mean fluorescent intensity (MFI) expression is depicted, unstained control is shown in gray. (B) Bar chart showing MFI of LC3B autophagy marker in *Glut1*-disrupted AML cells compared with cells transduced with nontargeting control. (C) Representative western blot and (D) its corresponding quantification of LC3B-I and LC3B-II. Data were normalized to expression in nontargeting control and to actin as a loading control (n = 2). (E) mRNA expression of *Atg7* in sorted GFP$^+$ (sgRNA-expressing) leukemia cells, 3 days after transduction, represented as FPKM values (n = 4). (F) Flow cytometric quantification of viable *MLL::AF9* cells transduced with *Glut1* sgRNAs or nontargeting control and then treated with dimethyl sulfoxide (DMSO) (vehicle) or 1 μM chloroquine (CQ) for 72 hours. Data were normalized to corresponding DMSO-treated controls, and statistics measured by unpaired 2-tailed Student *t* test. Data are shown as mean ± SD (n = 3) and statistical testing was performed by 1-way ANOVA, unless otherwise stated. *$P < .05$; **$P < .01$; ***$P < .001$; and ****$P < .0001$.

glucose uptake was impaired in a dose-dependent manner (Figure 6C). Consistent with the effects seen upon sgRNA-mediated *Glut1* knockdown, treatment of *MLL::AF9* leukemia cells with BAY-876 displayed a significantly larger amount of autophagic vacuoles (Figure 6D), and higher basal autophagy, as evidenced by an increased expression of the autophagy marker LC3B (supplemental Figure 5C). Notably, toward the higher concentrations, there were no indications of autophagy, correlating with an increased percentage of cells entering late-stage apoptosis (Figure 6E). Similar to what was observed for *Glut1* knockdown, BAY-876 treatment sensitized leukemia cells to chloroquine treatment, supporting that catabolic processes are induced as a prosurvival mechanism (Figure 6F).

Next, we examined the metabolic profile of *MLL::AF9* leukemia cells treated with the lower half-maximal inhibitory concentration (70 nM) of BAY-876 for 24 hours (Figure 6A; supplemental Figure 5D-I). Similar to genetically disrupting *Glut1*, the majority of glycolytic products, PPP metabolites, and TCA cycle intermediates were reduced in cells treated with BAY-876, suggesting a suppression of these pathways (supplemental Figure 5E-I; supplemental Table 5). In contrast to the sgRNA-mediated ablation of *Glut1*, BAY-876 treatment resulted in an overall reduction in amino acid levels (supplemental Figure 5E,I; supplemental Table 5). This discrepancy could potentially be because an earlier time point was measured for the pharmacological treatment, corroborating that metabolic patterns gradually shift over time.[34]

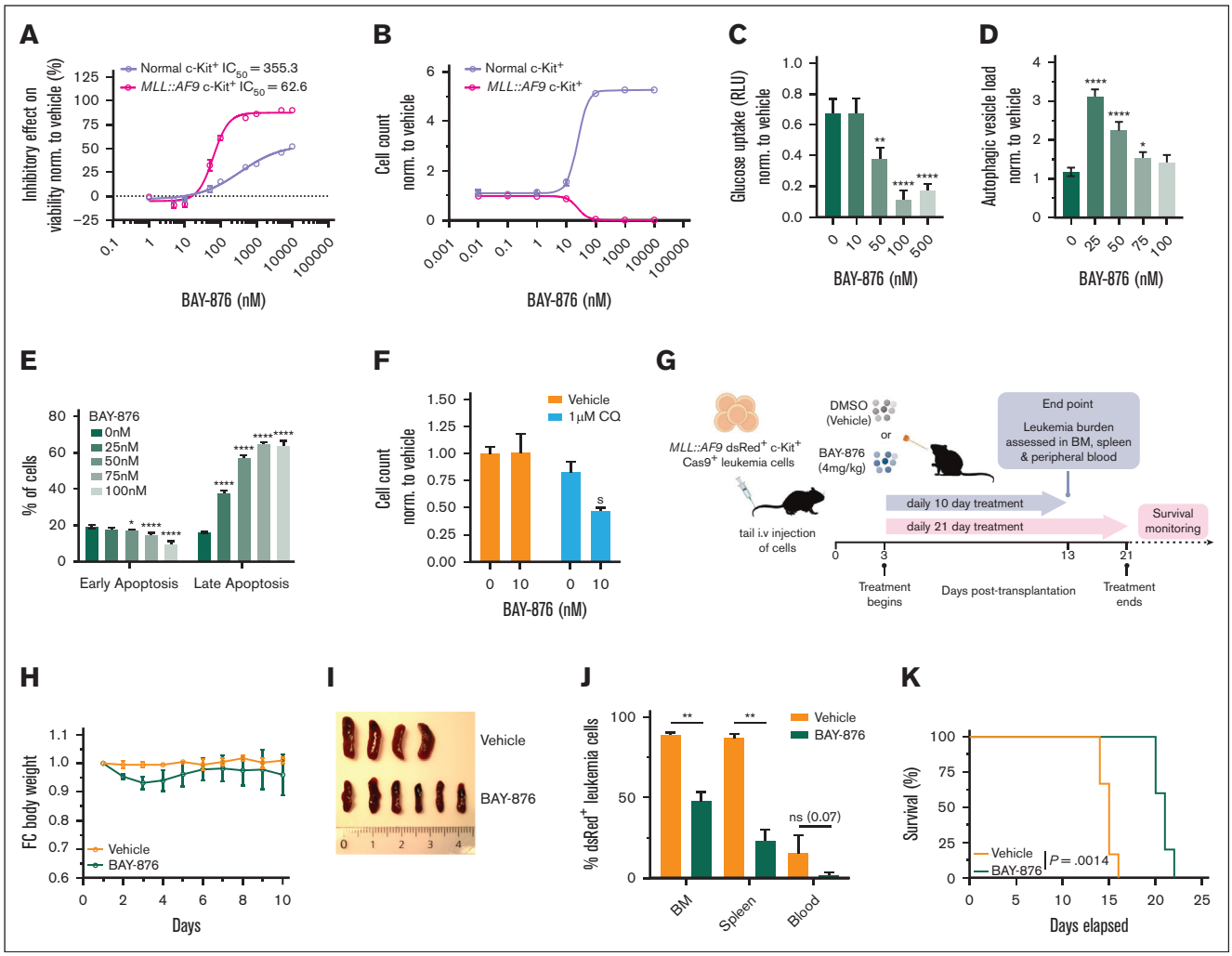

Figure 6. Pharmacological inhibition of GLUT1 by BAY-876 selectively targets *MLL::AF9* leukemia cells. (A) Dose-dependent inhibitory effect of 1-10 000 nM BAY-876 on c-Kit$^+$ normal and c-Kit$^+$ *MLL::AF9* leukemia cells assessed by total ATP levels after 24-hour treatment. The percentage of inhibition in viability is normalized to DMSO-treated controls, and IC_{50} values are indicated. (B) Flow cytometry quantification of cell numbers of normal and c-Kit$^+$ *MLL::AF9* leukemia cells upon 72-hour treatment with 0.01-10 000 nM BAY-876. (C-E) Dose-dependent effects on (C) glucose uptake, (D) autophagic vesicle load, and (E) early-/late-stage apoptosis status in *MLL::AF9* leukemia cells after 24- to 72-hour treatment with BAY-876. (F) Flow cytometric quantification of viable cells after 72-hour treatment with BAY-876 alone or 1 μM CQ. Data is normalized to DMSO-treated control, and synergistic effects are marked with the letter "S." (G) Schematic experimental outline for assessment of the inhibitory effect of BAY-876 on leukemia cells in vivo. For the experiment with a defined end point, mice received transplantation with 1×10^5 *MLL::AF9* c-Kit$^+$ cells, and 3 days after transplantation, were randomized into groups receiving daily dosing of 4 mg/kg BAY-876 or vehicle (n = 4-6 mice per group). After 10 days of treatment, animals were euthanized (end point) and leukemia burden was assessed. For the survival experiment, mice that received transplantation were treated with 4 mg/kg BAY-876 or vehicle for 21 days and monitored for survival (n = 5-6 mice per group). (H) Longitudinal comparison of body weight, (I) visual comparison of spleen size, and (J) percentage of leukemic occupancy in the BM, spleen, and peripheral blood of mice treated with BAY-876 or vehicle treatment. Significance was measured by unpaired 2-tailed Student *t* test. (K) Kaplan-Meier survival analysis of mice inoculated with c-Kit$^+$ *MLL::AF9* leukemia cells and treated with vehicle or BAY-876 for 21 days (n = 5-6 per group; log-rank test). Data are shown as mean ± SD (n = 3) and statistical testing was performed by 1-way ANOVA unless otherwise stated. *$P < .05$; **$P < .01$; and ****$P < .0001$. Illustration in panel G created using BioRender. Refer to supplemental Figure 5. ATP, adenosine triphosphate; BM, bone marrow; IC_{50}, half-maximal inhibitory concentration; RLU, relative luminescence units.

To evaluate the antileukemic effects of BAY-876 in vivo, we treated recipient mice that received transplantation with c-Kit$^+$ *MLL::AF9* leukemia cells with either BAY-876 or vehicle control via oral gavage (Figure 6G). The selected dose was well tolerated, resulting in minimal weight loss (Figure 6H). Mice treated with BAY-876 displayed reduced leukemic burden as evaluated by spleen weight (Figure 6I; supplemental Figure 5J), and presence of AML cells in the bone marrow, spleen, and peripheral blood (Figure 6J; supplemental Figure 5K). Notably, the antileukemic effects of BAY-876 also translated into prolonged survival from 18 to 24 days ($P = .0014$, Figure 6K). In agreement with the effects observed after genetic *Glut1* disruption, these findings provide further proof of concept that pharmacological targeting of GLUT1 in vivo has therapeutic efficacy in the *MLL::AF9* leukemia mouse model.

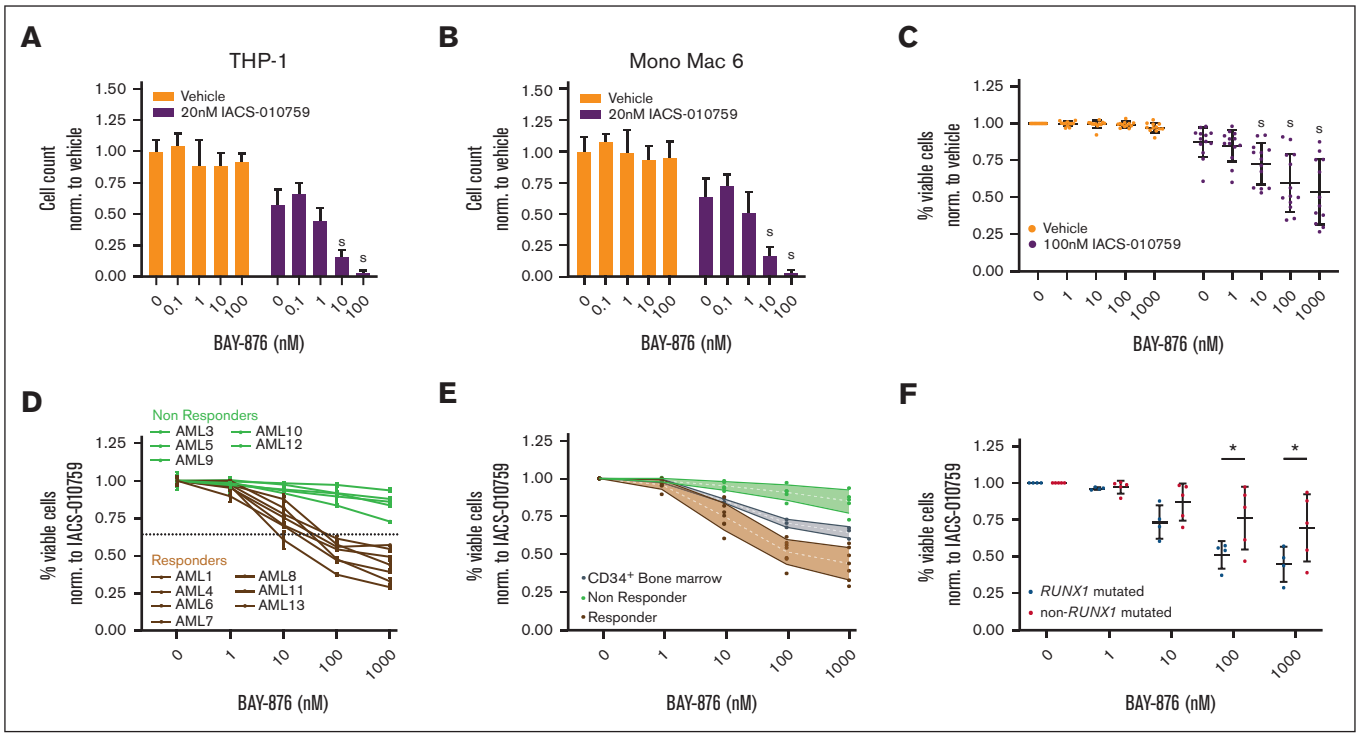

Figure 7. GLUT1 and OXPHOS inhibition has synergistic antileukemic efficacy in human AML cells. Assessment of synergistic effects between pharmacological inhibition of GLUT1 (BAY-876) and OXPHOS (IACS-010759) in (A) THP-1 and (B) Mono Mac 6. Quantification of viable cell counts after 72-hour treatment with increasing doses of BAY-876 alone (orange) or together with 20 nM IACS-010759 (purple) assessed by flow cytometry. Data were normalized to corresponding DMSO-treated controls. (C) Viability of primary AML samples treated ex vivo with indicated concentrations of BAY-876 alone (orange) or together with 100 nM IACS-010759 (purple), normalized to corresponding DMSO-treated controls. (D) Stratification of AML patients into "responders" and "nonresponders." (E) Viability of $CD34^+$ normal bone marrow cells relative to primary AML cells. (F) Comparison of viability in *RUNX1*-mutated vs wild-type adult AML after dual treatment with BAY-876 and 100 nM IACS-010759. (D-F) Data were normalized to viability corresponding to 100 nM IACS-010759 treatment alone and are shown as mean ± SD (n = 3-4). Synergistic effects have been marked with the letter "S." Statistical testing was performed by unpaired 2-tailed Student *t* test; $*P < .05$. Refer to supplemental Figures 6-9 and supplemental Table 4.

Dual GLUT1 and OXPHOS inhibition eliminates human AML cells by restraining metabolic reprogramming

Given the robust antileukemic effect of GLUT1 inhibition in murine LSCs, we evaluated whether human leukemia cells are dependent on GLUT1. A panel of AML cell lines with varying levels of GLUT1 was exposed to a range of BAY-876 concentrations, resulting in no obvious effect on growth inhibition (supplemental Figure 6A-B). In contrast to murine AML cells in which *Glut1* levels are predominant (supplemental Figure 2E), human AML cell lines (DepMap, Broad Institute) and samples from patients with AML from The Cancer Genome Atlas (TCGA) database had comparably high levels of *GLUT3* (supplemental Figure 6C-D).[38] Although the effect was variable, treatment with Glutor, an inhibitor targeting GLUT1, GLUT2, and GLUT3, only marginally affected cell viability of the tested AML cell lines (supplemental Figure 6E).[39] These findings argue against a redundancy between GLUT1 and GLUT3, and suggest that inhibition of the glucose transporters alone may not be sufficient to robustly suppress the growth of human AML cell lines.

One way in which cancer cells can metabolically adapt to limited glucose conditions is by rewiring to OXPHOS, allowing for the use of alternative nonglucose fuel sources to sustain their high metabolic needs.[40] To assess whether restraining their metabolic plasticity would enhance the antileukemic efficacy, we performed cotreatments with BAY-876 and the OXPHOS inhibitor IACS-010759, a mitochondrial electron transport chain inhibitor that has recently been evaluated in a phase 1 clinical trial in relapsed/refractory AML.[41,42] Human AML cell lines of varying subtypes (THP-1, KG-1, Mono Mac 6, and OCI-AML3) were treated with IACS-010759, BAY-876, or the combination. In contrast to BAY-876 treatment alone, cotreatment with IACS-010759 led to a strong synergistic dose-dependent reduced viability in all tested cell lines (supplemental Figure 6F; Figure 7A-B; supplemental Figure 7A-D). Replacing BAY-876 with Glutor in combination with IACS-010759 resulted in similar effects with only marginal improvement in the AML cell lines (supplemental Figure 7E-H). These findings demonstrate that OXPHOS inhibition sensitizes human AML cells to GLUT1 inhibition in a synergistic manner by restricting their metabolic plasticity.

To further explore the combination treatment, bulk primary AML cells isolated from the bone marrow of pediatric and adult patients with AML were used (n = 12; supplemental Table 4). Consistent with our observations in AML cell lines, BAY-876 and IACS-

010759 treatment had synergistic antileukemic effects in the majority of the primary AML samples, hereafter referred to as responders (Figure 7C-D; supplemental 8A-B). In the responders, which constituted 7 of 12 samples tested, the cotreatment had stronger antileukemic effects compared with those observed using $CD34^+$ normal bone marrow (Figure 7E; supplemental Figure 8C) and cord blood cells (supplemental Figure 8D-E), supportive of a therapeutic window.

Genomic examination revealed that all 4 samples from patients with *RUNX1*-mutated AML displayed strong sensitivity to the combination treatment (Figure 7F). Metabolic profiling of 3 *RUNX1*-mutated primary cells confirmed suppression of glycolysis and OXPHOS by BAY-876 and IACS-010759 treatment, respectively (supplemental Figure 8F-K). Of note, 1 patient sample exhibited increased glycolysis after IACS-010759 treatment alone, which was suppressed by the addition of BAY-876 (supplemental Figure 8F).

Next, by interrogation of the TCGA AML data set,[38] we sought to identify differential transcriptomic signatures between patients with *RUNX1*-mutated AML and those with non–*RUNX1*-mutated AML that could predict responsiveness to the combination treatment. *GLUT1* expression was comparable in wild type and *RUNX1*-mutated samples, in line with reports stating that GLUT1 expression levels do not predict sensitivity to GLUT1 inhibition (supplemental Figure 9A).[43] GSEA analysis revealed a negative enrichment of OXPHOS-related pathways in the *RUNX1*-mutated signature (supplemental Figure 9B).[44] This reduced OXPHOS state correlated with increased expression of pyruvate dehydrogenase kinase 1 (*PDK1*) and retinoblastoma tumor suppressor (*RB1*), reported to mediate a metabolic switch from OXPHOS to glycolysis (supplemental Figure 9C-D).[45-47]

Collectively, our findings suggest that combination of GLUT1 and OXPHOS inhibition is an effective antileukemic strategy for a large subset of patients with AML, in particular those belonging to the *RUNX1*-mutated AML subtype.

Discussion

Targeting metabolic dependencies in AML has therapeutic potential but effects are hampered by metabolic plasticity, the inherent or adaptive ability of cells to rewire their metabolic pathways.[6] In this study, GLUT1 was identified as an essential regulator of *MLL::AF9* LSCs in the bone marrow microenvironment by controlling energy metabolism. Inhibition of GLUT1 in LSCs induced autophagy and resulted in increased apoptosis and differentiation. Combined GLUT1 and OXPHOS inhibition eliminated human AML cells by reducing their metabolic plasticity.

Our findings show that GLUT1 inhibition suppresses glycolysis in murine LSCs, observations in agreement with recent reports in ovarian and breast cancer cell models.[45,48] As a metabolic adaptation to sustain energy demands when cellular bioenergetics were suppressed, we observed an increase in amino acid levels consistent with amino acids being a critical fuel source for LSCs.[49] Our findings suggest that in response to a disruption in GLUT1–mediated glucose uptake, AML cells induce autophagy as a mechanism to promote intracellular catabolism and nutrient recycling, thereby enabling the replenishment of amino acids.[34] Within the context of leukemia, autophagy has been reported to be critical to the survival of leukemia cells by acting as a positive regulator of OXPHOS when glycolysis is suppressed.[34,50]

Although these metabolic adaptations could partially compensate for the reduction in glucose uptake, it was insufficient to rescue the effect of *Glut1* disruption in *MLL::AF9* LSCs, which had lost their leukemia-initiating capacity when transplanted into mice. Both at a cellular and molecular level, we detected increased differentiation upon *Glut1* suppression, which could partially be related to downregulation of both *Hoxa9* and *Meis1*, key factors in regulating the self-renewal and differentiation of LSCs in *MLL*-rearranged AML.[17,33]

Our finding that inhibition of GLUT1 by BAY-876 led to a suppression of leukemic burden and prolonged survival of mice is in agreement with the anticancer effects reported for BAY-876 in ovarian and breast cancer models.[45,48] Interestingly, LSCs residing in the hypoglycemic bone marrow niche upregulate AMP–activated protein kinase (AMPK), which in turn induces GLUT1 expression, highlighting GLUT1 as a therapeutic target in vivo.[51] This pro-survival adaptation lends further support to the therapeutic value of inhibiting GLUT1, because this would prevent the adaption of LSCs to the metabolic stress in the hypoglycemic niche.

Unlike in murine *MLL::AF9* LSCs, BAY-876 treatment or simultaneous inhibition of GLUT1-3 with Glutor did not exert potent cytotoxic effects on human AML cells. This lack of response to blocked glucose import is consistent with observations that human AML cells, LSCs in particular, depend on other sources of fuel such as amino acids and fatty acids that are metabolized through OXPHOS.[49,52-54] Furthermore, to adapt to glycolysis suppression caused by limiting glucose conditions, several cancer types upregulate mitochondrial functions and increase reliance on OXPHOS to meet adenosine triphosphate (ATP) demands.[34] Notably, we found that OXPHOS inhibition sensitized both AML cell lines and samples from patients with AML to GLUT1 inhibition, suggesting that suppressing OXPHOS increases the dependency on alternative energy sources such as glycolysis that can be therapeutically exploited. Furthermore, the lactate-suppressive ability of BAY-876 that we, and others, have reported may help mitigate the neurotoxic effects associated with elevated lactate levels recently reported for IACS-010759 treatment in patients with AML.[42,45,48] These findings highlight the value of simultaneously targeting multiple metabolic pathways to synergistically suppress AML cell growth and overcome therapy resistance caused by metabolic reprogramming, but future validations of these findings using human LSCs are needed.

We observed synergistic antileukemic efficacy with the combination treatment in a broad range of AML subtypes, particularly in *RUNX1*-mutated primary AML samples. Notably, *RUNX1*-mutated AML exhibited markedly higher expression of *RB1* and *PDK1*, which are biomarkers of a glycolysis-biased metabolism and may highlight a subgroup that would benefit from GLUT1-directed therapies.[44,46,47]

In conclusion, we demonstrate that inhibition of GLUT1 eliminates murine *MLL::AF9* LSCs by reducing intracellular bioenergetics and inducing myeloid differentiation and apoptosis. As a result of limiting glucose import, amino acids are supplied through autophagy as a metabolic adaptation. Dual inhibition of GLUT1 and

OXPHOS acts synergistically to counteract metabolic reprogramming in human AML. These findings strengthen our understanding of the metabolic dependencies of AML cells, thus offering a rationale for new combinatorial metabolism-directed therapeutic strategies in AML.

Acknowledgments

The authors thank the Swedish Cancer Society, the Swedish Childhood Cancer Foundation, the Medical Faculty of Lund University, the Swedish Research Council, governmental funding of clinical research within the National Health Services, Sweden, and the European Union's (EU) Horizon 2020 research and innovation program under the Marie Skłodowska-Curie Action (MSCA) grant agreement EU-MSCA-COFUND-754299 for supporting this work. The Swedish Metabolomics Centre, Umeå, Sweden (www.swedishmetabolomicscentre.se) is acknowledged for conducting metabolic profiling. Bioinformatic support was provided by the Computational Analytics Support Platform, Umeå, Sweden.

Authorship

Contribution: M.J., M.R.-Z., and R.R. conceived the study and designed the experiments; M.R.-Z., K.R., S.G., R.R., L.O., T.F., K.B., M.E., P.P.-M., N.P.-M., H.L., J.C., C.J.P., and V.L performed experiments, and analyzed and interpreted the data; M.J. and M.R.-Z. wrote the first draft of the manuscript; M.J., M.R.-Z., T. F., A.K.H.-A., and N.-B.W. reviewed and edited the manuscript; and M.J. acquired funding.

Conflict-of-interest disclosure: The authors declare no competing financial interests.

ORCID profiles: L.O., 0000-0003-0130-6602; A.F.-C., 0000-0002-5341-4472; P.P.-M., 0000-0002-0789-6431; N.P.-M., 0000-0002-5996-2349; C.J.P., 0000-0002-0073-9660; A.K.H.-A., 0000-0002-2904-1311; N.-B.W., 0000-0001-6052-922X; M.J., 0000-0003-4080-7055.

Correspondence: Marcus Järås, Division of Clinical Genetics, Lund University, Klinikgatan 28, BMC C13, 22184 Lund, Sweden; email: marcus.jaras@med.lu.se.

References

1. Shallis RM, Wang R, Davidoff A, Ma X, Zeidan AM. Epidemiology of acute myeloid leukemia: recent progress and enduring challenges. *Blood Rev*. 2019;36:70-87.
2. Shlush LI, Mitchell A, Heisler L, et al. Tracing the origins of relapse in acute myeloid leukaemia to stem cells. *Nature*. 2017;547(7661):104-108.
3. Pollyea DA, Gutman JA, Gore L, Smith CA, Jordan CT. Targeting acute myeloid leukemia stem cells: a review and principles for the development of clinical trials. *Haematologica*. 2014;99(8):1277-1284.
4. Jones CL, Inguva A, Jordan CT. Targeting energy metabolism in cancer stem cells: progress and challenges in leukemia and solid tumors. *Cell Stem Cell*. 2021;28(3):378-393.
5. Mishra SK, Millman SE, Zhang L. Metabolism in acute myeloid leukemia: mechanistic insights and therapeutic targets. *Blood*. 2023;141(10):1119-1135.
6. Grønningsæter IS, Reikvam H, Aasebø E, et al. Targeting cellular metabolism in acute myeloid leukemia and the role of patient heterogeneity. *Cells*. 2020;9(5), 1155-1126.
7. Ramakrishnan R, Peña-Martínez P, Agarwal P, et al. CXCR4 signaling has a CXCL12-independent essential role in murine MLL-AF9-driven acute myeloid leukemia. *Cell Rep*. 2020;31(8):107684.
8. Bajaj J, Hamilton M, Shima Y, et al. An in vivo genome-wide CRISPR screen identifies the RNA-binding protein Staufen2 as a key regulator of myeloid leukemia. *Nat Cancer*. 2020;1(4):410-422.
9. Lin S, Larrue C, Scheidegger NK, et al. An in vivo CRISPR screening platform for prioritizing therapeutic targets in AML. *Cancer Discov*. 2022;12(2):432-449.
10. Bausch-Fluck D, Hofmann A, Bock T, et al. A mass spectrometric-derived cell surface protein atlas. *PLoS One*. 2015;10(3):e0121314.
11. Peña-Martínez P, Eriksson M, Ramakrishnan R, et al. Interleukin 4 induces apoptosis of acute myeloid leukemia cells in a Stat6-dependent manner. *Leukemia*. 2018;32(3):588-596.
12. Sanjana NE, Shalem O, Zhang F. Improved vectors and genome-wide libraries for CRISPR screening. *Nat Methods*. 2014;11(8):783-784.
13. Chapellier M, Peña-Martínez P, Ramakrishnan R, et al. Arrayed molecular barcoding identifies TNFSF13 as a positive regulator of acute myeloid leukemia-initiating cells. *Haematologica*. 2019;104(10):2006-2016.
14. Miller PG, Al-Shahrour F, Hartwell KA, et al. In vivo RNAi screening identifies a leukemia-specific dependence on integrin beta 3 signaling. *Cancer Cell*. 2013;24(1):45-58.
15. Tavor S, Petit I, Porozov S, et al. CXCR4 regulates migration and development of human acute myelogenous leukemia stem cells in transplanted NOD/SCID mice. *Cancer Res*. 2004;64(8):2817-2824.
16. Majeti R, Chao MP, Alizadeh AA, et al. CD47 is an adverse prognostic factor and therapeutic antibody target on human acute myeloid leukemia stem cells. *Cell*. 2009;138(2):286-299.
17. Faber J, Krivtsov AV, Stubbs MC, et al. HOXA9 is required for survival in human MLL-rearranged acute leukemias. *Blood*. 2009;113(11):2375-2385.
18. Zhang D, Wang Q, Zhu T, et al. RACK1 promotes the proliferation of THP1 acute myeloid leukemia cells. *Mol Cell Biochem*. 2013;384(1-2):197-202.

19. Li N, Yang Y, Liang C, et al. Tmem30a plays critical roles in ensuring the survival of hematopoietic cells and leukemia cells in mice. *Am J Pathol*. 2018;188(6):1457-1468.
20. Rapin N, Bagger FO, Jendholm J, et al. Comparing cancer vs normal gene expression profiles identifies new disease entities and common transcriptional programs in AML patients. *Blood*. 2014;123(6):894-904.
21. Svendsen JB, Baslund B, Cramer EP, Rapin N, Borregaard N, Cowland JB. MicroRNA-941 expression in polymorphonuclear granulocytes is not related to granulomatosis with polyangiitis. *PLoS One*. 2016;11(10):e0164985.
22. Taskesen E, Bullinger L, Corbacioglu A, et al. Prognostic impact, concurrent genetic mutations, and gene expression features of AML with CEBPA mutations in a cohort of 1182 cytogenetically normal AML patients: further evidence for CEBPA double mutant AML as a distinctive disease entity. *Blood*. 2011;117(8):2469-2475.
23. Wouters BJ, Löwenberg B, Erpelinck-Verschueren CAJ, van Putten WLJ, Valk PJM, Delwel R. Double CEBPA mutations, but not single CEBPA mutations, define a subgroup of acute myeloid leukemia with a distinctive gene expression profile that is uniquely associated with a favorable outcome. *Blood*. 2009;113(13):3088-3091.
24. Metzelder SK, Michel C, Von Bonin M, et al. NFATc1 as a therapeutic target in FLT3-ITD-positive AML. *Leukemia*. 2015;29(7):1470-1477.
25. Klein HU, Ruckert C, Kohlmann A, et al. Quantitative comparison of microarray experiments with published leukemia related gene expression signatures. *BMC Bioinformatics*. 2009;10:422.
26. Kohlmann A, Kipps TJ, Rassenti LZ, et al. An international standardization programme towards the application of gene expression profiling in routine leukaemia diagnostics: the Microarray Innovations in LEukemia study prephase. *Br J Haematol*. 2008;142(5):802-807.
27. Bagger FO, Kinalis S, Rapin N. BloodSpot: a database of healthy and malignant haematopoiesis updated with purified and single cell mRNA sequencing profiles. *Nucleic Acids Res*. 2019;47(D1):D881-D885.
28. Andersson AK, Ma J, Wang J, et al. The landscape of somatic mutations in infant MLL-rearranged acute lymphoblastic leukemias. *Nat Genet*. 2015;47(4):330-337.
29. Subramanian A, Tamayo P, Mootha VK, et al. Gene set enrichment analysis: a knowledge-based approach for interpreting genome-wide expression profiles. *Proc Natl Acad Sci U S A*. 2005;102(43):15545-15550.
30. Marchwicka A, Marcinkowska E. Regulation of expression of CEBP genes by variably expressed vitamin D receptor and retinoic acid receptor α in human acute myeloid leukemia cell lines. *Int J Mol Sci*. 2018;19(7):1918.
31. Lubbert M, Miller CW, Koeffler HP. Changes of DNA methylation and chromatin structure in the human myeloperoxidase gene during myeloid differentiation. *Blood*. 1991;78(2):345-356.
32. Collins CT, Hess JL. Role of HOXA9 in leukemia: dysregulation, cofactors and essential targets. *Oncogene*. 2016;35(9):1090-1098.
33. Kumar AR, Hudson WA, Chen W, Nishiuchi R, Yao Q, Kersey JH. Hoxa9 influences the phenotype but not the incidence of Mll-AF9 fusion gene leukemia. *Blood*. 2004;103(5):1823-1828.
34. Shiratori R, Furuichi K, Yamaguchi M, et al. Glycolytic suppression dramatically changes the intracellular metabolic profile of multiple cancer cell lines in a mitochondrial metabolism-dependent manner. *Sci Rep*. 2019;9(1):18699.
35. Kandasamy P, Gyimesi G, Kanai Y, Hediger MA. Amino acid transporters revisited: new views in health and disease. *Trends Biochem Sci*. 2018;43(10):752-789.
36. Klionsky DJ, Abdalla FC, Abeliovich H, et al. Guidelines for the use and interpretation of assays for monitoring autophagy. *Autophagy*. 2012;8(4):445-544.
37. Siebeneicher H, Cleve A, Rehwinkel H, et al. Identification and optimization of the first highly selective GLUT1 inhibitor BAY-876. *ChemMedChem*. 2016;11(20):2261-2271.
38. Cancer Genome Atlas Research Network, Ley TJ, Miller C, Ding L, et al. Genomic and epigenomic landscapes of adult de novo acute myeloid leukemia. *N Engl J Med*. 2013;368(22):2059-2074.
39. Reckzeh ES, Karageorgis G, Schwalfenberg M, et al. Inhibition of glucose transporters and glutaminase synergistically impairs tumor cell growth. *Cell Chem Biol*. 2019;26(9):1214-1228.e25.
40. Anderson NM, Mucka P, Kern JG, Feng H. The emerging role and targetability of the TCA cycle in cancer metabolism. *Protein Cell*. 2018;9(2):216-237.
41. Molina JR, Sun Y, Protopopova M, et al. An inhibitor of oxidative phosphorylation exploits cancer vulnerability. *Nat Med*. 2018;24(7):1036-1046.
42. Yap TA, Daver N, Mahendra M, et al. Complex I inhibitor of oxidative phosphorylation in advanced solid tumors and acute myeloid leukemia: phase I trials. *Nat Med*. 2023;29(1):115-126.
43. Åbacka H, Hansen JS, Huang P, et al. Targeting GLUT1 in acute myeloid leukemia to overcome cytarabine resistance. *Haematologica*. 2021;106(4):1163-1166.
44. Yokota A, Huo L, Lan F, Wu J, Huang G. The clinical, molecular, and mechanistic basis of RUNX1 mutations identified in hematological malignancies. *Mol Cells*. 2020;43(2):145-152.
45. Wu Q, Ba-alawi W, Deblois G, et al. GLUT1 inhibition blocks growth of RB1-positive triple negative breast cancer. *Nat Commun*. 2020;11(1):4205.
46. Erdem A, Marin S, Pereira-Martins DA, et al. The glycolytic gatekeeper PDK1 defines different metabolic states between genetically distinct subtypes of human acute myeloid leukemia. *Nat Commun*. 2022;13(1):1105.

47. Suresh Babu V, Dudeja G, SA D, et al. Lack of retinoblastoma protein shifts tumor metabolism from glycolysis to OXPHOS and allows the use of alternate fuels. *Cells*. 2022;11(20):3182.

48. Ma Y, Wang W, Idowu M, et al. Ovarian cancer relies on glucose transporter 1 to fuel glycolysis and growth: anti-tumor activity of BAY-876. *Cancers (Basel)*. 2018;11:33.

49. Jones CL, Stevens BM, D'Alessandro A, et al. Inhibition of amino acid metabolism selectively targets human leukemia stem cells. *Cancer Cell*. 2018; 34(5):724-740.e4.

50. Kawaguchi M, Aoki S, Hirao T, Morita M, Ito K. Autophagy is an important metabolic pathway to determine leukemia cell survival following suppression of the glycolytic pathway. *Biochem Biophys Res Commun*. 2016;474(1):188-192.

51. Saito Y, Chapple RH, Lin A, Kitano A, Nakada D. AMPK protects leukemia-initiating cells in myeloid leukemias from metabolic stress in the bone marrow. *Cell Stem Cell*. 2015;17(5):585-596.

52. Lagadinou ED, Sach A, Callahan K, et al. BCL-2 inhibition targets oxidative phosphorylation and selectively eradicates quiescent human leukemia stem cells. *Cell Stem Cell*. 2013;12(3):329-341.

53. Sriskanthadevan S, Jeyaraju DV, Chung TE, et al. AML cells have low spare reserve capacity in their respiratory chain that renders them susceptible to oxidative metabolic stress. *Blood*. 2015;125(13):2120-2130.

54. Stevens BM, Jones CL, Pollyea DA, et al. Fatty acid metabolism underlies venetoclax resistance in acute myeloid leukemia stem cells. *Nat Cancer*. 2020; 1(12):1176-1187.